J Comp Physiol A (1984) 154:367–380

Journal of Comparative Physiology A Sensory, Neural, and Behavioral Physiology

Neural control of the hearts in the leech, *Hirudo medicinalis*

I. Anatomy, electrical coupling, and innervation of the hearts

Anthony R. Maranto and Ronald L. Calabrese*
The Biological Laboratories, Harvard University, 16 Divinity Avenue Cambridge, Massachusetts 02138, USA

Accepted December 12, 1983

Summary. 1. The longitudinal and circular muscle fibers observed in cross sections of the hearts of *Hirudo medicinalis* are different regions of a single type of spindle shaped muscle cell. The cells are arranged with their thin tapering arms running longitudinally along the lumen of the heart and their thick central regions forming the perimeter of the heart.

2. Two geometrical forms of these cells exist: a *cis* form whose arms project longitudinally in the same direction, and a *trans* form whose arms project in opposite directions.

3. The *cis* and *trans* forms are differentially distributed along the heart in a pattern which repeats in every segment. This differential distribution may contribute to the formation of the sphincter in each segment.

4. Heart muscle cells are electrically coupled. The length constant for passive electrotonic spread of current along the heart is approximately 0.6 mm. Intracellularly injected Lucifer yellow also passes into adjacent cells.

5. Muscle cells form contacts by sending microvilli to adjacent cells. Large patches of particles resembling E face gap junctions are seen with freeze fracture electron microscopy.

6. Two classes of central neurons, heart excitor motor neurons (HE cells) and heart accessory neurons (HA cells), innervate the heart. Both neurons make classical chemical junctions with heart muscle cells as seen with the electron microscope.

7. HE cells evoke excitatory junctional potentials in heart muscle cells while HA cells do not. The roles of these cells in controlling the polarization and constriction of the heart are described in the second and third papers of this series (Maranto and Calabrese 1984; Calabrese and Maranto 1984).

Introduction

The leech heartbeat has proved to be extremely useful for studying the control of movement because every stage of the heartbeat circuit is accessible to anatomical and physiological examination. Beginning with the work of Thompson and Stent (1976a, b, c) which demonstrated that the constriction pattern of the leech's two hearts is controlled by a set of interneurons and motor neurons in the central nervous system, considerable progress has been made toward elucidating the neural mechanisms which produce the heartbeat program (for a recent review see Calabrese and Peterson 1983). In this and the following two papers we report additional properties of the central and peripheral heartbeat circuit which affect the execution of the central program by the heart.

In the circulatory system of the leech, *Hirudo medicinalis*, blood is pumped through a closed system of vessels by two lateral vessels, called heart tubes or hearts. The hearts run longitudinally along the entire length of the animal and communicate with other non-contractile blood vessels through a segmentally repeating set of three smaller contractile side branches (Gaskell 1914). Blood generally flows anteriorly through the hearts and returns posteriorly through passive dorsal and ventral longitudinal sinuses. There is also considerable side-to-side blood flow which is apparently aided by one sphincter in each segment of the heart tube itself and one at the insertion of each side branch (Boroffka and Hamp 1969; Thompson and

* To whom offprint requests should be sent

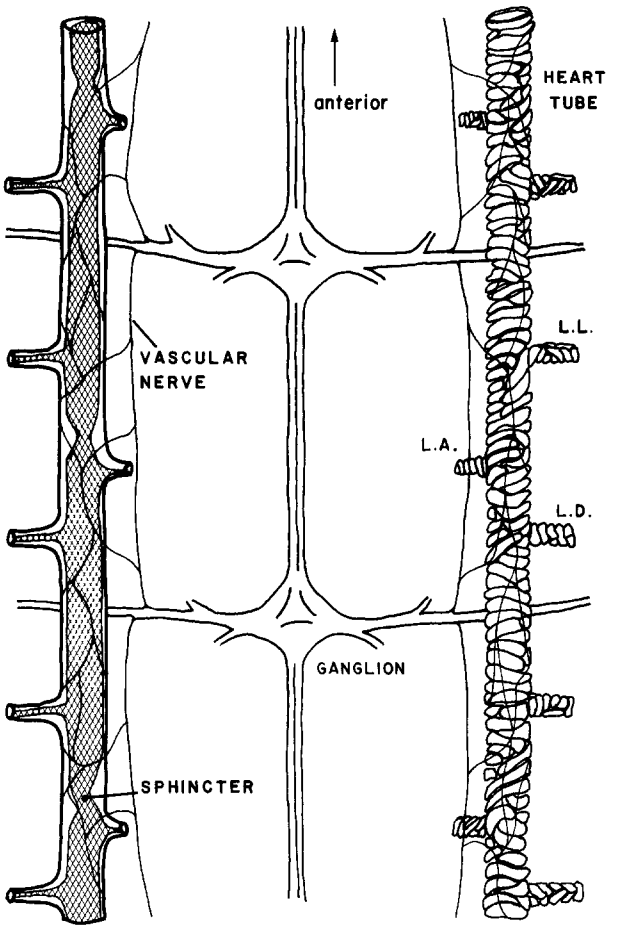

Fig. 1. Schematic drawing of the relationship between the ventral nerve cord and lateral hearts. Side branches of the heart are abbreviated: *L.L.* latero-lateral; *L.A.* latero-abdominal; *L.D.* latero-dorsal. On the left the heart is drawn in outline with the lumen stippled. On the right the outlines of the individual heart muscle cells are drawn. Ganglia and hearts are not drawn to the same scale

Stent 1976a). Figure 1 is a schematic representation of the hearts and side branches in two body segments.

The wall of each heart consists of an outer layer of circular muscle fibers and an inner layer of longitudinal muscle fibers. Since the work of Gaskell (1914) at the light microscope level and of Hammersen and Staudte (1969) at the electron microscope level, it has been assumed that the fibers in these two layers are somatically distinct from each other. In this paper we demonstrate that the longitudinal and circular fibers are merely different regions of a single type of spindle-shaped muscle cell. The spiral forms of these cells apparently contribute to the shape of the heart wall and the efficient constriction of the heart.

In the following paper we show that individual heart muscle cells can produce a polarization rhythm (Maranto and Calabrese 1984). Electrical coupling reported in this paper probably synchronizes the myogenicity of individual muscle cells in the intact heart tube.

Two types of neurons influence the myogenic activity of the heart. Heart excitor motor neurons (HE cells) phasically coordinate activity along the heart (Thompson and Stent 1967a; Maranto and Calabrese 1984) while heart accessory neurons (HA cells) regulate myogenic period and beat tension (Calabrese and Maranto 1984). In this paper we show that both types of neurons form conventional synapses with heart muscle cells.

Methods

Animals. Hirudo medicinalis were purchased from European suppliers and were maintained in aerated aquaria at 15–20 °C for up to 4 months before use.

Physiological solutions. Dissections and physiological recordings were usually performed with the preparation bathed in normal physiological saline (Nicholls and Baylor 1968) containing (in mmol/l) 115 NaCl, 4 KCl, 1.8 $CaCl_2$, 10 glucose, and 10 Tris buffer adjusted to pH 7.4. Preparations to be maintained for several days were bathed in Leibovitz's L-15 culture medium (Gibco) (pH 7.4) with 2% fetal bovine serum (Gibco), 10 mg/ml gentamycin sulfate, and 0.6% glucose (Fuchs et al. 1981).

Dissection. The hearts were removed by a dorsal dissection for anatomical studies or for the isolation of muscle cells described in the following paper (Maranto and Calabrese 1984). To trace central neuronal projections out to the heart with dye injections, body segments were dissected and pinned as described for in situ preparations in the following paper (Maranto and Calabrese 1984). For physiological recording and dye injection the heart was isolated. Nylon monofilament fishing line (2 pound test) was inserted through a nick in the heart and run through the lumen for a few segments. Surrounding connective tissue was then removed and a piece of heart was isolated from the animal by cutting through the heart and monofilament at two points. The heart was stretched to its original length (the length of the monofilament) and pinned in a clear Sylgard-coated plastic dish. Isolating and pinning the heart with the monofilament in its lumen greatly facilitated intracellular recording from the muscle cells by preventing constriction of the heart tube.

Intracellular recording. All recordings were made at room temperature, 20–25 °C, with standard microelectrodes filled with 4 mol/l potassium acetate.

Intracellular dye injection and processing for microscopy. Cells to be injected with dyes were first identified with standard recording microelectrodes and then reimpaled with dyefilled micropipettes.

Lucifer yellow CH (Stewart 1978) was injected iontophoretically or with pressure. Injected specimens were prepared for fluorescence microscopy by immersing them in 50% glycerol in saline and mounting them between a slide and cover glass.

Cells were viewed and photographed with a Zeiss Universal microscope equipped with 200 W mercury lamp whose beam was filtered by a BG12 exciter filter and a 530 nm interference filter. Fluorescence was filtered through barrier filter 53 and photographed with Ektachrome 400 film.

Pressure was used to inject cells with horseradish peroxidase (HRP) (Muller and McMahan 1976). Injection micropipettes were filled with 2% HRP (Sigma Type VI). 0.2% Fast Green in 0.2 mol/l KCl. Before injection the tips of the pipettes were either touched lightly to the bottom of the recording dish or bevelled on a rotating piece of alumina paper (0.2 μm grit).

To allow the HRP to diffuse from the somata of central neurons to the heart tube, preparations were kept at 4 °C in L-15 medium for 4–5 days after injection. Then the heart tubes and ganglia were removed and fixed in ice-cold 2% glutaraldehyde, 2% formaldehyde in 0.1 mol/l Na cacodylate buffer, pH 7.4, for 3 h. The preparations were then rinsed and allowed to soak overnight in buffer. A reaction product was formed by immersing the preparations in 0.05% 3,3′-diaminobenzidine tetrahydrochloride (DAB; Sigma) and 0.01% hydrogen peroxide in cacodylate buffer. When the cell bodies and processes were visibly stained, the preparations were washed with several changes of buffer.

Wholemounts were made for light microscopy by dehydrating the tissue through a graded series of ethanols, clearing it in methyl benzoate and xylenes, and mounting it between a slide and coverslip with Permount.

Tissue was prepared for electron microscopy by post-fixation with 1% osmium tetroxide in 0.1% Na cacodylate buffer, pH 7.4, for 1 h at room temperature. The tissue was then rinsed 3 times with buffer, dehydrated through ethanols and propylene dioxide, and embedded in Epon resin. Thin sections were cut with a diamond knife, mounted on copper grids, and viewed at 80 kV with a Philips 300 electron microscope.

A few muscle cells in the heart were stained by intracellular iontophoresis of cobalt (10% $CoCl_2$ in distilled water) (Pitman et al. 1971). The cobalt was precipitated with 1% ammonium sulfide in saline, and fixed for 1 h with 2% glutaraldehyde in 0.1 mol/l Na cacodylate buffer, pH 7.4. After washing, the cobalt precipitate was further intensified by the Timm's method modified by Bacon and Altman (1977). The heart was dehydrated through ethanols and propylene oxide, embedded in Epon, and serially sectioned at 5 μm with glass knives. Reconstructions of injected cells were made from camera lucida drawings.

Extracellular staining of the heart tube. Isolated sections of heart tube were soaked in 2% HRP in saline for an hour or more. The hearts were then processed as described above for whole mount preparation of HRP injected cells.

Freeze fracture. Heart tubes were fixed in ice-cold 2% glutaraldehyde in 0.1 mol/l Na cacodylate buffer for 15 min, washed several times with buffer, and allowed to equilibrate in a solution of 20% glycerol in cacodylate buffer. Small pieces of tissue were mounted on copper or gold disks and rapidly plunged into a slush of Freon cooled by liquid nitrogen. The tissue was fractured in a Balzers device at −110 °C and 2×10^{-6} Torr followed immediately by platinum shadowing at 45 °C and deposition of carbon at 90 °C. The resulting replicas were cleaned with household bleach, washed with distilled water, and mounted on copper grids. Replicas were examined and photographed at 80 kV with a Philips electron microscope. The freeze fracture photographs which appear in this paper were printed with reserve contrast compared to the appearance of the replicas.

Results

General structure of the heart

With the aid of a phase contrast microscope or an extracellular stain, the structure of the heart was examined in wholemount preparations. Figure 2a shows the external surface of a 0.1 mm length of heart stained extracellularly with horseradish peroxidase (HRP). This piece represents only about 2% of the length of each tube per body segment. As previously described by Gaskell (1914) and Hammersen and Staudte (1969), the outer surface of the heart consists of closely fitting muscle fibers arranged nearly circularly around the tube. The visible part of each muscle fiber wraps almost halfway around the circumference of the tube. Each fiber is 10–15 μm thick at its widest part.

In electron microscopic cross section, the wall of the heart is seen to contain a layer of longitudinal muscle fibers between the outer circular fibers and the endothelial lining of the lumen (Fig. 2b; also Hammersen and Staudte 1969). The longitudinal fibers are of smaller diameter (1–10 μm) than the circular fibers. The cells are surrounded by an external matrix which is devoid of other cell types except for axon bundles and microvilli of unknown origin. The ultrastructure of the muscle fibers, axons, and endothelial cells is described in great detail by Hammersen and Staudte (1969).

Shapes of muscle cells

Are muscle fibers in the circular and longitudinal layers truly distinct? Previous workers (Gaskell 1914; Hammersen and Staudte 1969) concluded that they were distinct on the basis of reconstruction from sections. To view the shapes of the cells in wholemount, we injected muscle cells in the circular layer with horseradish peroxidase (Fig. 3a). This dye does not cross membranes or gap junctions (Muller and McMahan 1976; Muller and Carbonetto 1979). Not only is the circular region in the area of the injection stained, but so are two longitudinal processes which originate at either end of the circular region. These processes run beneath the circular layer for distances up to 200 μm until they taper down to fine endings.

Every injected cell possessed a circular region and two longitudinal arms, but the arms did not always follow the same course. Figure 3b shows two muscle cells filled with Lucifer yellow by pressure injection. The cell on the left has essentially the same form as the HRP injected cell in Fig. 3a; that is, the longitudinal arms extend in opposite

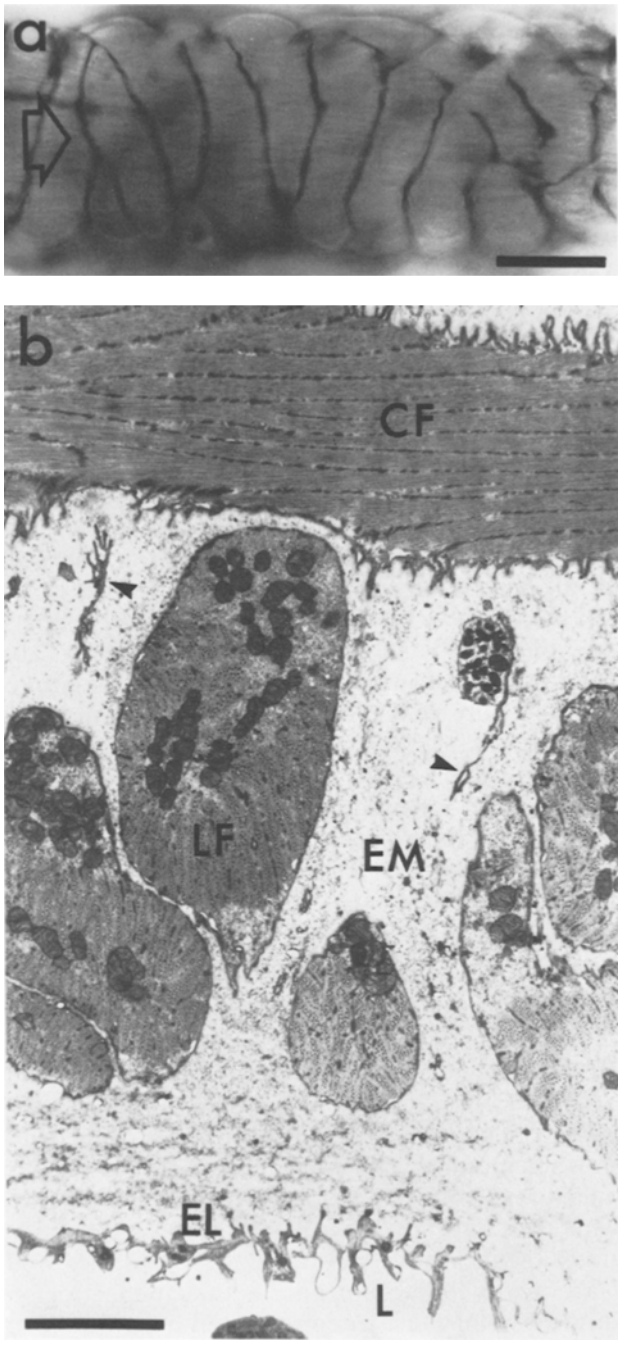

Fig. 2a, b. Anatomy of the heart. **a** Outer surface of a heart which was stained extracellularly with horseradish peroxidase to enhance the borders between muscle cells. The hollow arrow indicates the longitudinal axis of the heart. Scale bar, 20 μm. **b** Electron micrograph of a cross section through the wall of the heart. *CF* circular muscle fiber; *LF* longitudinal muscle fiber; *EM* extracellular matrix; *EL* layer of endothelial cells; *L* lumen; arrowheads, microvilli of uncertain origin. Scale bar, 3 μm

directions. The cell on the right extends both arms in the same direction. These two forms of cell are called *trans* and *cis*, respectively. Except for the direction of their branching patterns, the dimensions of the *cis* and *trans* forms are similar.

From the dye injections we concluded that the fibers in the circular and longitudinal layers are simply different regions of a single type of muscle cell. We also examined suspensions of heart muscle cells after they had been isolated by enzymatic dispersion of the heart to determine their structure. All of the isolated muscle cells in such a preparation appear similar (Fig. 3c). They are about 10 μm wide in the center with long tampering ends. Their length (100–200 μm) is shorter than expected from the combined lengths of the circular and longitudinal regions, but this discrepancy is probably due to contraction and damage during isolation.

To trace the course of a muscle fiber through the wall of the heart, a cobalt filled cell was serially thick sectioned and graphically reconstructed from camera lucida drawings. Such a reconstruction is shown in Fig. 3d. As is typical for both *cis* and *trans* cells, the longitudinal arms of this *cis* cell project to the opposite side of the lumen after leaving the circular region. Often, as is the case for this cell, the arms of *cis* cells crossed over each other about midway along their length. Therefore, the overall shape of a *cis* cell may be interpreted as a spiral which doubles back on itself. The shape of a *trans* cell is essentially a normal spiral.

Distribution of cis and trans forms

The distribution of muscle cell forms along a segment of heart was investigated by randomly injecting 122 muscle cells in four hearts with Lucifer yellow. The insertion points of the side branching vessels were used to divide the segment into three regions (Fig. 4A). Thus, region (a) lies between the latero-lateral and latero-dorsal branches, region (b) between the latero-dorsal and latero-abdominal branches, and region (c) between the latero-abdominal and latero-lateral branches. Injected cells were tallied with respect to: (1) their location in one of these regions, (2) their form (*cis* or *trans*), and (3) the direction of their arms if of the *cis* form (anterior or posterior projecting). The lower half of Fig. 4A summarizes the data as the percentages of each form of cell detected out of the total number of cells injected *within* one region. For example, out of the 56 cells injected in region (a), 27 *trans* cells (40%) were detected.

There was no significant difference (chi-square test) between the total number of *cis* cells and the

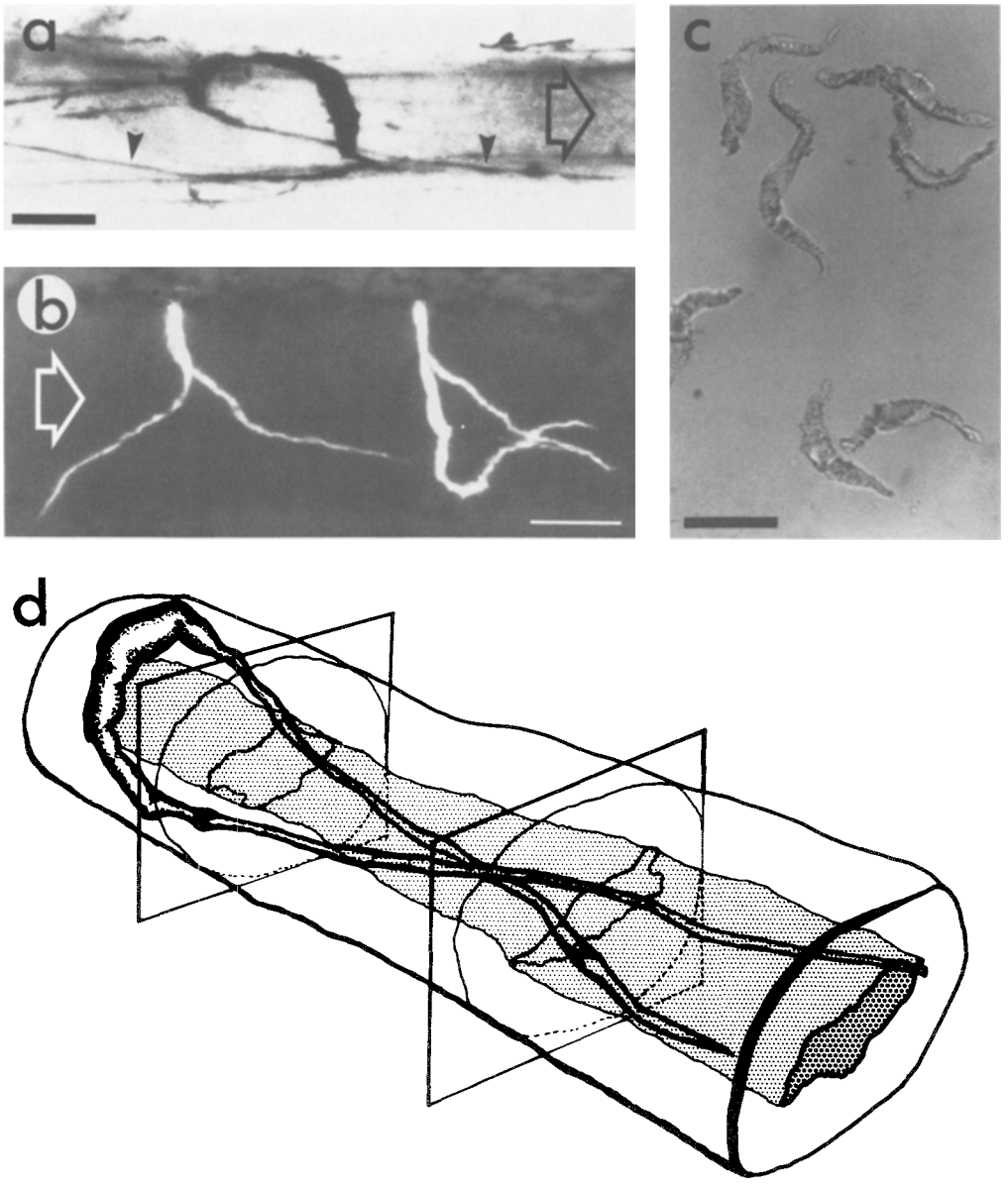

Fig. 3a–d. Structure of heart muscle cells. **a** A muscle cell stained with horseradish peroxidase. Arrowheads point to the longitudinal arms of the cell. The hollow arrow indicates the longitudinal axis of the heart. Scale bar, 30 μm. **b** Two muscle cells that were pressure-injected with Lucifer yellow. The cell on the left is of the *trans* form while the one on the right is of the *cis* form. The hollow arrow indicates the longitudinal axis of the heart. Scale bar, 50 μm. **c** Muscle cells isolated by enzymatic dissociation of the heart. Scale bar, 40 μm. **d** Reconstruction of a *cis* muscle cell which had been stained with cobalt and sectioned

number of *trans* cells in a given region. That is, the percentages of *cis* and *trans* cells in a region are approximately equal. Additionally, the percentages of anterior and posterior projecting *cis* cells in region (a) were also approximately equal. However, in region (b) the anterior projecting *cis* cells greatly outnumbered the posterior projecting *cis* cells ($P<0.001$). In region (c) the posterior projecting *cis* cells were in the majority ($P<0.0005$). Clearly, the arms of the *cis* cells in regions (b) and (c) preferentially point toward an area between the two regions.

One would expect that the extra longitudinal arms from *cis* cells between regions (b) and (c) would lead to a thickening of the heart wall. Indeed, this is the region of the previously described valve (Gaskell 1914), or sphincter (Boroffka and Hamp 1969). To predict crudely the amount of thickening which might be expected from the extra longitudinal arms, we calculated values for 'predicted relative arm overlap' at three points *between* regions (a), (b), and (c). These values (Fig. 4A, B) are simply sums of the percentages of cells which send their arms toward points (c–a), (a–b),

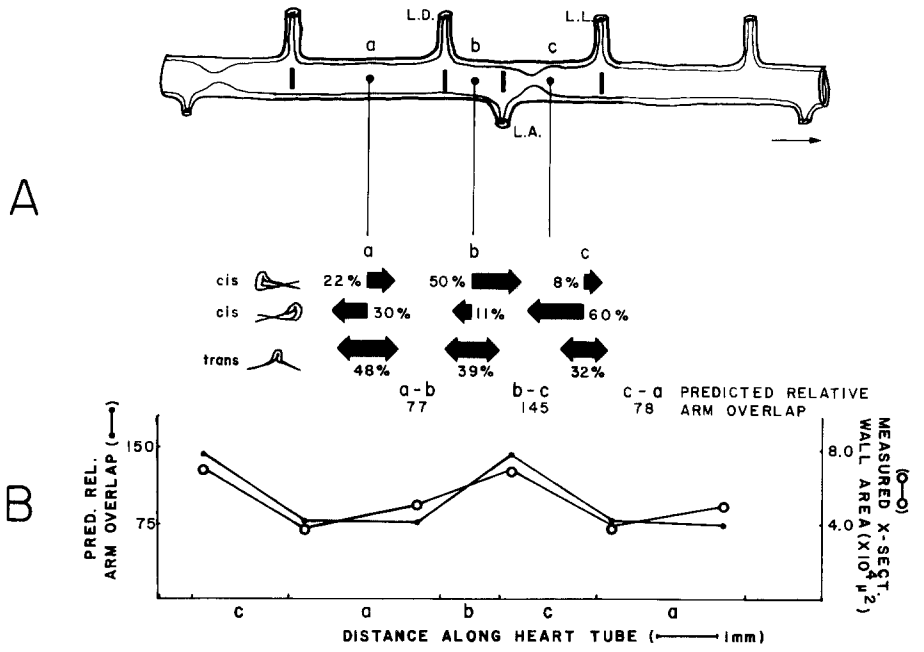

Fig. 4A, B. Analysis of *cis* and *trans* muscle cell distribution. **A** Schematic of the heart with side branches referenced as in Fig. 1. The percentages of each form of muscle cell in three regions between the side branches are indicated below each region. Total number of cells counted in regions a, b, and c were 56, 28, and 38 respectively. Muscle cell forms were identified by staining with Lucifer yellow. Cells of the *cis* form were divided into two groups depending on the direction of their arms. The small arrow points anteriorly. Predicted relative arm overlap at three points along the heart was calculated by summing the percentages of each form of muscle cell which sent arms into that region. **B** Graphic comparison of the predicted relative arm overlap (solid dots) from A and actual measurements of the cross-sectional area (clear dots) of the heart at the three points indicated. Data are repeated at either end of the graph

and (b–c). Percentages of *trans* cells were divided in half before summation because only one of their arms projects toward the same point. For example, the calculation for point (b–c) is $50+60+(39/2)+(32/2)=145$. Figure 4B illustrates that there is a twofold increase in the predicted relative arm overlap in the region of the sphincter (b–c) compared to other regions. Actual data of the cross sectional area of the heart wall are superimposed on the same graph to illustrate the relative amount of thickening at the sphincter. The area measurements were made by sectioning a heart tube, tracing the outlines of the wall with a camera lucida, and then weighing cut-outs of the tracings. Comparison of the true area data with the predicted relative arm overlap calculations suggests that the sphincter thickening is at least partly due to the additional *cis* cell arms in that region.

Other cell forms

Although all of the muscle cells are of the *cis* or *trans* forms, slight variations in these forms are also found at specializations along the heart. One variation occurs in the region of the sphincter. Cells with their circular portions in this region tend to be thinner and shorter than cells elsewhere along the heart. As a result of their reduced length, the arms of these cells do not extend out of the sphincter region (Fig. 5a). Another variation, also principally one of size, occurs in the side branches. *Cis* and *trans* cells in these vessels are miniature versions of the cells in the main vessel (Fig. 5b).

Dye coupling

When heart muscle cells were injected with Lucifer yellow using current rather than pressure, dye often spread into adjacent muscle cells (Fig. 6a). The number of stained adjacent cells was extremely variable ranging from 0 to over 10.

Contacts between muscle cells

Hammersen and Staudte's (1969) finding that heart muscle cells are always separated from each other by at least the thickness of their basement membrane is inconsistent with dye or electrical coupling. Therefore, we reexamined the heart by injecting muscle cells with HRP to look for contacts between injected and uninjected cells. Fig-

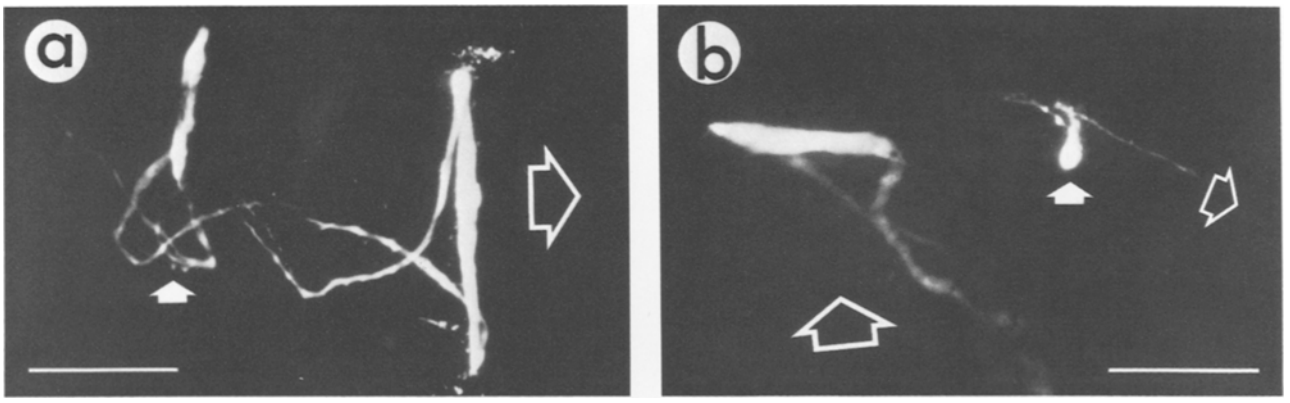

Fig. 5a, b. Additional forms of muscle cells. **a** The white arrow points to a Lucifer yellow stained cell in the region of the sphincter. A nearby *cis* cell was also stained for comparison. The hollow arrow indicates the longitudinal axis of the heart. Scale bar, 50 μm. **b** A muscle cell in a side branch (white arrow) and a typical muscle cell in the main tube stained with Lucifer yellow. Large and small hollow arrows indicate the longitudinal axes of the heart and side branch, respectively. Scale bar, 50 μm

ure 6b shows such a contact. Contacts are made by fine processes which leave the main body of the injected cell and come to rest beneath the basement membrane of adjacent muscle cells. At these points the plasma membranes of the two cells run parallel with an extracellular gap of about 10 nm. The plasma membrane of the uninjected cell appears to stain more densely in these regions than elsewhere along its surface. Along some areas the extracellular gap appears to be obliterated. No other specializations associated with the membranes were noticeable at these contacts.

The discovery of fine processes connecting muscle cells probably also accounts for the observation of microvilli in the extracellular matrix and on the surface of muscle cells (Fig. 2b).

Gap junctions and Z-element attachment sites

Gap junctions have been reported between electrically coupled cells in both vertebrates and invertebrates (Bennett and Goodenough 1978). Because gap junctions are readily visualized by freeze fracture electron microscopy, the leech heart was subjected to this technique. When heart muscle membranes were fractured (Fig. 6c, d), the external leaflet (E face) revealed large patches of particles which resembled E face gap junctions found in other annelids and arthropods (Gilula 1974; Flower 1977; Larsen 1977). The patches were distributed randomly in the muscle membrane. Their shapes were irregular and their sizes were comparable with the sizes of muscle cell contacts such as those in Fig. 6b (0.2–0.3 μm). Particles within these patches were 11–14 nm in diameter.

Another class of particles was also found on the E face (Fig. 6c). These particles were in small circular clusters with diameters of approximately 60 nm. The clusters occurred in rectilinear arrays with 0.4–0.7 μm spacing. Additionally, each cluster sat upon a small convexity in the membrane. Particles within these small clusters were somewhat smaller and more uniform in size (10–12 nm) than particles in the large patches. Because these clusters are approximately the same size and are arranged in the same rectilinear manner as intracellular filament bundles known as Z-elements (Hammersen and Staudte 1969), they may represent attachment sites for Z-elements.

Specializations on the cytoplasmic leaflet (P face) were difficult to detect because of the high concentration of particles on this face (Fig. 6e). However, linear arrays of concavities were present with similar size and spacing as the small convexities on the E face.

Electrical coupling

Electrical coupling among muscle cells in the heart was investigated by inserting microelectrodes into three cells along lengths of heart (Fig. 7A). Current was injected through one electrode and the spread of current into other cells was detected as voltage changes at the other electrodes. All three electrodes could be used for either current injection or voltage recording. Figure 7B illustrates the results of injecting constant amplitude and duration depolarizing or hyperpolarizing current pulses into each of three cells separated by distances indicated in Fig. 7A. As shown in the right half of Fig. 7B, hyperpolarizing current injected into any cell passively spreads in either direction along the heart. Depolarizing current could also be observed to flow in either direction and, in this instance,

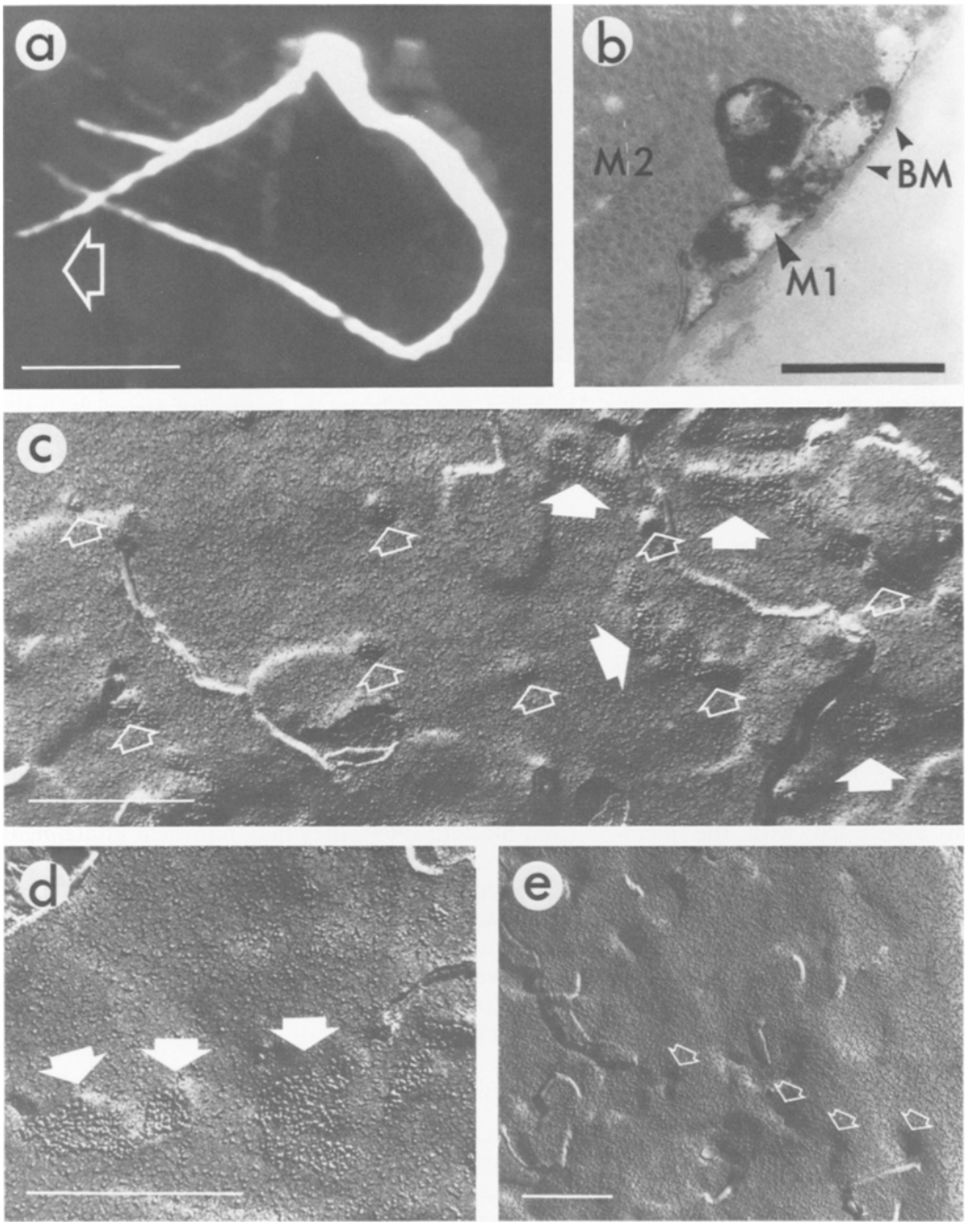

Fig. 6a–e. Anatomical evidence for coupling between heart muscle cells. **a** A muscle cell stained with Lucifer yellow iontophoretically. Faint fluorescence is also visible in other muscle cells into which the dye has spread. The arrow indicates the longitudinal axis of the heart. Scale bar, 50 μm. **b** Electron micrograph showing processes (M1) from a muscle cell stained with horseradish peroxidase contacting an unstained muscle cell (M2) beneath its basement membrane (*BM*). Scale bar, 0.5 μm. **c** Freeze fracture replica of the E face of a muscle cell showing a linear array of small clusters of particles (hollow arrows) and the random appearance of large patches of particles (white arrows). Each small cluster of particles is associated with a convexity. The large patches probably correspond to gap junctions while the small clusters probably correspond to attachment sites for Z-elements (see text). Scale bar, 0.5 μm. **d** Large patches of particles on the E face of a muscle cell. Scale bar, 0.5 μm. **e** P face of a muscle cell showing uniform high density of particles. Hollow arrows indicate a linear arrangement of concavities. Scale bar, 0.5 μm

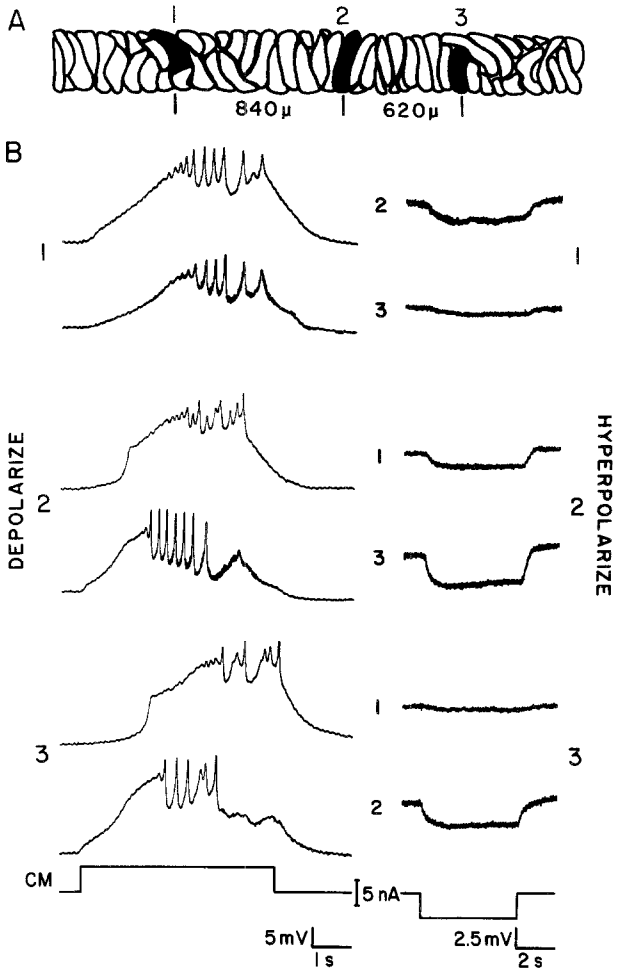

Fig. 7A, B. Electrical coupling along the heart. **A** Schematic drawing of the heart indicating the distances between 3 muscle cells impaled with microelectrodes. **B** Intracellular recordings from pairs of muscle cells when the third muscle cell was depolarized (left) or hyperpolarized (right). Numbers down left and right edges indicate the cell that was injected with current. Numbers down center indicate the cells from which the recordings were made. *CM* Current monitor

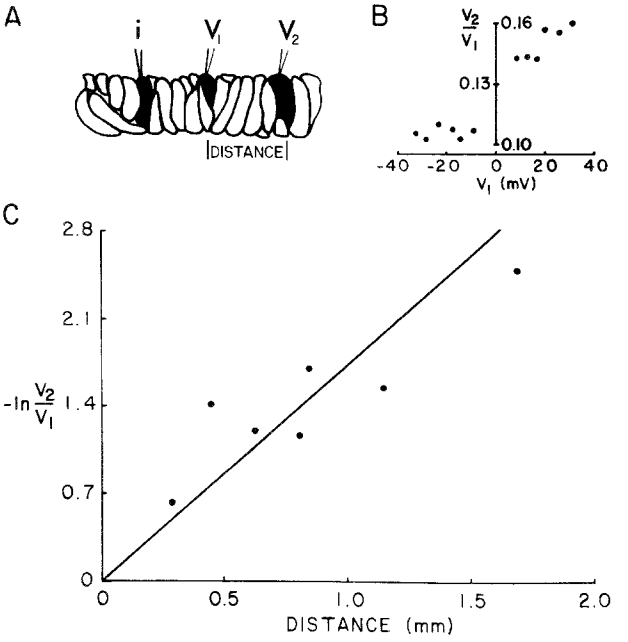

Fig. 8A–C. Length constant of the heart. **A** Schematic drawing indicating the placement of intracellular electrodes for length constant determinations. Current was injected at electrode i and voltages were measured at electrodes V1 and V2 separated by Distance. **B** Coupling coefficient (V2/V1) vs voltage at V1 for a typical preparation illustrating that coupling coefficient is relatively independent of the magnitude of the test pulse for hyperpolarizing currents but not for depolarizing currents. **C** Plot of $-\ln(V2/V1)$ vs Distance for seven different pieces of heart. Each point represents one measurement at one distance. The reciprocal of the slope of the hand fitted line represents the average length constant (0.57 nm)

a depolarizing current pulse into any cell initiated an active response which propagated along the heart in both directions (left half of Fig. 7B). These results indicate that the muscle cells of the heart are electrically coupled and that such coupling may allow mutual excitation between muscle cells.

The degree of electrical coupling between two cells is often represented by the coupling coefficient, V2/V1, where V1 is a voltage displacement applied to one cell and V2 is the attenuated voltage measured in the other cell. In a linear arrangement of coupled cells, coupling coefficients between cells at increasing distances are expected to decrease exponentially. The rate of exponential decay can be represented by a single value, the length constant, defined as the distance over which an applied voltage displacement is attenuated by a factor of 1/e.

Figure 8A illustrates the placement of electrodes for length constant determinations. Length constants were determined from the equation:

Length Constant = Distance/-ln (V2/V1).

Figure 8B contains a sample of coupling coefficients (V2/V1) from a single preparation in which hyperpolarizing and depolarizing currents of various magnitudes were used to produce a voltage V1. These data demonstrate the stability of coupling coefficient measurements for hyperpolarizing pulses compared to depolarizing pulses for this preparation. Depolarizing currents presumably activate voltage sensitive conductances which alter the apparent coupling. To avoid the effects of such voltage dependent conductances, only hyperpolarizing current pulses were used to determine length constants.

For seven heart preparations taken from three leeches, length constant measurements ranged between 0.31 and 0.75 nm.The mean of these seven

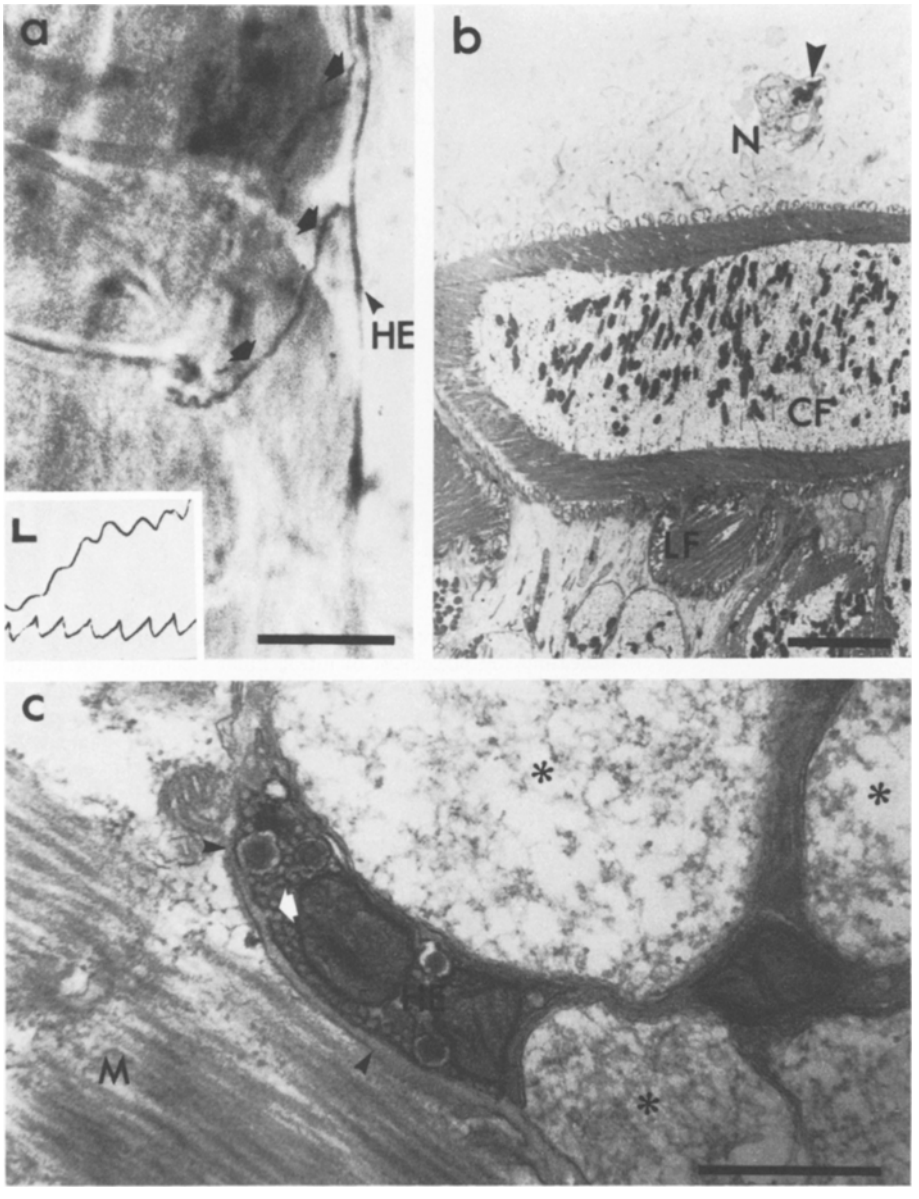

Fig. 9a–c. Horseradish peroxidase labeled processes of an HE cell on the heart.
a A nerve containing an HRP stained process (HE) from an HE cell running along the heart. Solid arrows indicate HRP stained branches which leave the nerve. Scale bar, 10 μm. Inset: Excitatory junctional potentials in a heart muscle cell (upper trace) match one-for-one with action potentials in an HE cell (lower trace). Vertical scale: upper trace, 2 mV; lower trace, 10 mV. Horizontal scale: 100 ms.
b Electron micrograph of a cross section through a nerve (N) running along the heart. The nerve contains a single HRP stained axon of an HE cell (arrowhead). *CF* circular region of a muscle fiber; *LF* longitudinal region of a muscle fiber. Scale bar, 5 μm.
c Electron micrograph of an HRP stained terminal of an HE cell (*HE*) forming a synapse (between arrowheads) with a muscle cell (*M*) in the heart. White arrow indicates a vesicle fused with the presynaptic membrane. Asterisk marks processes of cells of undetermined origins. Scale bar, 0.5 μm

values was 0.57 mm or approximately 10% of the length of the heart tube in one segment. The scatter of these measurements about the mean is indicated in Figure 8C, which is a graph of the seven values of $-\ln(V2/V1)$ at the various distances they were determined. The slope of the diagonal line is the reciprocal of the mean length constant.

Innervation of the heart by identified neurons

Action potentials in the HE motor neuron produce discrete excitatory junctional potentials in heart muscle cells in normal external calcium concentrations (1.8 mmol/l) (Inset, Fig. 9a) as well as in elevated calcium concentrations (20 mmol/l) (Thompson and Stent 1976a). We examined the heart for processes from the HE motor neuron by injecting HE cell bodies with HRP and letting the dye diffuse to the periphery by keeping the preparation in culture for 4–5 days. In four of the six preparations examined, HRP filled processes were found along the heart (Fig. 9a). When material from these preparations was sectioned for electron microscopy, label was found localized in axons (Fig. 9b) and axon terminals forming neuromuscular junctions (Fig. 9c). Axon terminals contained clear synaptic vesicles approximately 50 nm in diameter and large dense core vesicles 80–120 nm in diameter. Mitochondria were also present. The junctional cleft was occupied by the basement

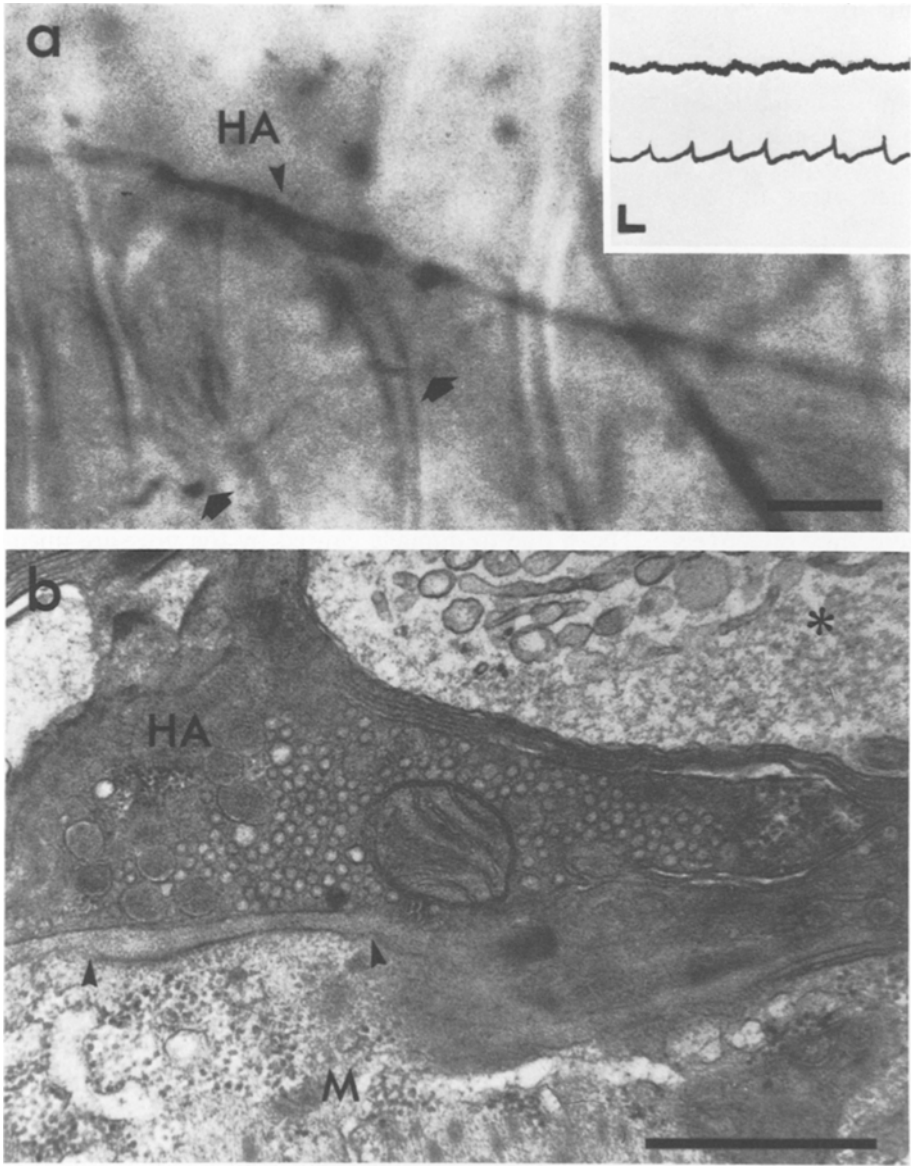

Fig. 10a, b. Horseradish peroxidase labeled processes of an HA cell on the heart.
a An HRP stained axon of an HA cell (*HA*) running over the surface of the heart. Solid arrows point to a branch which leaves the larger axon. Scale bar, 10 μm. Inset: Action potentials in the HA cell (lower trace) do not give rise to junctional potentials in a heart muscle cell (upper trace). Vertical scale: upper trace, 2 mV; lower trace, 10 mV. Horizontal scale, 100 ms.
b Electron micrograph of an HRP stained terminal of an HA cell (*HA*) forming a synapse (between arrowheads) with a muscle cell (*M*) in the heart. Asterisk indicates a process of unknown origin. Scale bar, 0.5 μm

membrane and was 50–60 nm thick. The postjunctional membrane often had filamentous material associated with it.

As we demonstrate in the third paper of this series, the HA cell modulates the myogenic activity of the heart (Calabrese and Maranto 1984). Spikes in the HA cell do not elicit junctional potentials in heart muscle cells (Inset, Fig. 10a). In the same muscle cell recorded in the Inset of Fig. 10a the innervating HE motor neuron elicited summating excitatory junctional potentials both immediately before and after the record shown, indicating that the muscle cell was not damaged. In fact the spike activity of the innervating HE cell had to be transiently suppressed by intracellular injection of hyperpolarizing current to obtain the record shown.

When we searched for HA cell processes on the heart by injecting HA cell bodies with HRP, we found in two separate preparations that the HA cell projected to the heart (Fig. 10a). Labeled axon terminals forming junctions directly with heart muscle cells were also present (Fig. 10b). The ultrastructural characteristics of these junctions were indistinguishable from those of HE cell junctions.

Discussion

Construction of the heart

All of the muscle cells in the heart are fundamentally spiral. The 'double-belted' construction of the heart wall results from the thick central regions

of the spirals encircling their thin arms. Variations in the wall thickness are achieved by the existence of *cis* spirals which send both arms in the same direction in addition to *trans* spirals which are normal spirals. At the sphincter in every segment the heart wall is thicker because of the presence of additional *cis* cells extending their arms into this area.

The dynamic consequence of constructing the heart from spiral cells is that radial and longitudinal contractions are always coupled. Observation of contracting hearts verifies this prediction. The benefit derived from coupling constriction with shortening is the greater systolic pressure developed by combining these actions than by using either alone. Spiral muscles with similar actions (oblique muscles) are also present in the body wall of the leech (Mann 1962). There they effectively increase the hydrostatic pressure of the body to enable the leech to assume a rigid posture.

Electrical coupling

Extensive electrical coupling is usually a feature of systems where synchrony is important (Bennett 1974). The leech circulatory system is an interesting case where synchrony is important only half of the time. Constrictions of the leech's two hearts are coordinated via the HE cells by the heartbeat central pattern generator so that one heart constricts peristaltically while the other heart constricts synchronously. Every 20 to 50 heartbeats the pattern switches sides (Thompson and Stent 1976a; Calabrese 1977). Thus, strong electrical coupling is only advantageous while a heart is in the synchronous mode. Strong coupling would be detrimental to peristalsis if it allowed excitation to spread electrotonically along the heart faster than neural excitation. At present we do not have values for the conduction velocity of electrotonically propagated excitation because we were able to induce a propagating depolarization in only one experiment over a distance too short to measure conduction velocity (Fig. 7B). However, since the hearts do follow the central pattern, we must assume that the electrical coupling is not sufficient to produce synchrony among adjacent segments. The fact that the length constant is only 10% of the length of one segment strengthens this conclusion.

While electrical coupling may not be strong enough to synchronize adjacent segments, it undoubtedly synchronizes cells over shorter distances. For example, in Fig. 7B the patterns of spikes in cells 2 and 3 were nearly identical when cell 1 was depolarized. Such coupling over short distances may serve to synchronize the bursting activity of muscle cells in the heart (Maranto and Calabrese 1984).

Dye coupling

Diffusion of Lucifer yellow between electrically coupled cells was first observed by Stewart (1978) in the retina. Shortly thereafter, Muller and Scott (1979) demonstrated Lucifer yellow coupling between electrically coupled neurons in the leech. Therefore, it is likely that Lucifer yellow coupling between heart muscle cells is also mediated through electrotonic junctions. The lack of dye coupling when Lucifer yellow was injected with pressure rather than iontophoretically may have been due to damage caused by the pressure injection pipettes.

Gap junctions

The large patches of particles seen on the E face of freeze fracture replicas are likely candidates for gap junctions. In contrast with vertebrate gap junctions whose particles are found on the P face (Bennett and Goodenough 1978), the particles of many annelid and arthropod gap junctions are found on the E face (Flower 1977). Some E face gap junction particles are regularly spaced as in the crayfish (Peracchia 1973) while others in annelids and insects are not (Satir and Gilula 1973; Gilula 1974; Flower 1977; Larsen 1977). The heterogeneous size and irregular spacing of these particles in the leech heart are comparable to the sizes and spacings of gap junction particles in the guts of insects (Satir and Gilula 1973) and earthworms (Larsen 1977).

Recently Pumplin and Muller (1983) found P face gap junction particles in the muscle cells of the leech connectives. Citing studies in which tissues were fixed or unfixed, they suggested that fixation may account for the variability in which face the particles are found. Since they fixed for 2 h while we fixed for 15 min, the differences between the gap junctions in connective muscle and heart muscle may also be related to fixation.

Innervation

Since HRP does not cross membranes or gap junctions (Muller and McMahan 1976; Muller and Carbonetto 1979), the finding of HRP labeled junctions on the heart is conclusive evidence for monosynaptic contacts by HE motor neurons and HA neurons on the heart. Terminals with similar

appearances have been described previously in the leech on the muscles of the body wall (Rosenbluth 1973; Yaksta-Sauerland and Coggeshall 1973), the muscles in the central nervous system (Tulsi and Coggeshall 1971), and the heart (Hammersen and Staudte 1969). Neuromuscular junctions in *Lumbricus* also have the same appearance (Mill and Knapp 1970).

Small clear vesicles and large dense core vesicles such as those seen in the HE and HA cells are characteristics of cholinergic terminals found at frog neuromuscular junctions (Heuser and Reese 1974) and sympathetic ganglia (Dickinson-Nelson and Reese 1983). The cholinergic nature of the HE cell neuromuscular junction is also supported by: (1) the detection of significant amounts of choline acetylase and acetylcholinesterase in the HE cell body (Wallace 1981a, b; Wallace and Gillon 1982), (2) the ability of iontophoretically and bath applied ACh (10 nanomolar) to depolarize eserinized heart muscle (Maranto 1983), and (3) the ability of curare to block depolarization produced by HE cell discharges and exogenously applied ACh (Maranto 1983).

In the following two papers we will show that the HE cell entrains myogenic bursting of the heart while the HA cell has chronotropic and inotropic modulatory effects on myogenic bursting (Maranto and Calabrese 1984; Calabrese and Maranto 1984). The HE cell mediates its effects by eliciting excitatory junctional potentials in muscle cells while the HA cell does not affect the membrane potential of muscle cells to achieve its effects. In light of these findings it is perhaps surprising that the HE and HA cell terminals are structurally indistinguishable.

Acknowledgements. We thank C.S. Cozzens for editorial assistance. Supported by grants from the National Science Foundation (BNS 81-08837 and BNS 81-21551).

References

Bacon JP, Altman JS (1977) A silver intensification method for cobalt filled neurones in wholemount preparations. Brain Res 138:359–363

Bennett MVL (1974) Flexibility and rigidity in electrotonically coupled systems. In: Bennett MVL (ed) Synaptic transmission and neuronal interaction. Raven Press, New York, pp 153–178

Bennett MVL, Goodenough DA (1978) Gap junctions, electrotonic coupling, and intercellular communication. Neurosci Res Prog Bull 16:373–486

Boroffka I, Hamp R (1969) Topographie des Kreislaufsystems und Zirkulation bei: *Hirudo medicinalis*. Z Morphol Tiere 64:59–76

Calabrese RL (1977) The neural control of alternate heartbeat coordination states in the leech, *Hirudo medicinalis*. J Comp Physiol 122:111–143

Calabrese RL, Maranto AR (1984) Neural control of the hearts in the leech, *Hirudo medicinalis* III. Regulation of myogenicity and muscle tension by heart accessory neurons. J Comp Physiol A 154:393–406

Calabrese RL, Peterson E (1983) Neural control of heartbeat in the leech, *Hirudo medicinalis*. Symp Soc Exp Biol (in press)

Dickinson-Nelson A, Reese TS (1983) Structural changes during transmitter release at synapses in the frog sympathetic ganglion. J Neurosci 3:42–52

Flower NE (1977) Invertebrate gap junctions. J Cell Sci 25:163–171

Fuchs PA, Nicholls JG, Ready DF (1981) Membrane properties and selective connexions of identified leech neurones in culture. J Physiol 316:203–223

Gaskell JF (1914) The chromaffine system of annelids and the relation of this system to the contractile vascular system in the leech, *Hirudo medicinalis*. A contribution to the comparative physiology of the contractile vascular system and its regulators, the adrenaline secreting system and the sympathetic nervous system. Philos Trans R Soc Lond 205B:153–211

Gilula NB (1974) Junctions between cells. In: Cox RP (ed) Cell communication. John Wiley and Sons, New York, pp 1–29

Hammersen F, Staudte HW (1969) Beiträge zum Feinbau der Blutgefäße von Invertebraten. I. Die Ultrastruktur des Sinus lateralis von *Hirudo medicinalis* L. Z Zellforsch 100:215–250

Heuser JE, Reese TS (1974) Morphology of synaptic vesicle discharge and reformation at the frog neuromuscular junction. In: Bennett MVL (ed) Synaptic transmission and neuronal interaction. Raven Press, New York, pp 59–77

Larsen WJ (1977) Structural diversity of gap junctions. Tissue Cell 9:373–394

Mann H (1962) Leeches (Hirudinea). Their structure, physiology, ecology and embryology. Pergamon Press, New York

Maranto AR (1983) The roles of neuronal and muscular properties in generating the leech heartbeat. PhD dissertation, Harvard University, Cambridge MA

Maranto AR, Calabrese RL (1984) Neural control of the hearts in the leech, *Hirudo medicinalis* II. Myogenic activity and its control by heart motor neurons. J Comp Physiol A 154:381–391

Mill PJ, Knapp MF (1970) Neuromuscular junctions in the body wall muscles of the earthworm, *Lumbricus terrestris* L. J Cell Sci 7:263–271

Muller KJ, Carbonetto S (1979) The morphological and physiological properties of a regenerating synapse in the CNS of the leech. J Comp Neurol 185:485–516

Muller KJ, McMahan UJ (1976) The shapes of sensory and motor neurones and the distribution of their synapses in ganglia of the leech: A study using intracellular injection of horseradish peroxidase. Proc R Soc London Ser B 194:481–499

Muller KJ, Scott SA (1979) Correct axonal regeneration after target cell removal in the central nervous system of the leech. Science 206:87–89

Nicholls JG, Baylor DA (1968) Specific modalities and receptive fields of sensory neurons in the CNS of the leech. J Neurophysiol 31:740–756

Peracchia C (1973) Low resistance junctions in crayfish. II. Structural details and further evidence for intercellular channels by freeze fracture and negative staining. J Cell Biol 57:66–76

Pitman RM, Tweedle MJ, Cohen MJ(1971) Branching of central neurons: Intracellular cobalt injection for light and electron microscopy. Science 176:412–414

Pumplin DW, Muller KJ (1983) Distinctions between gap junctions and sites of intermediate filament attachment in the leech C.N.S. J Neurocytol 12:805–815

Rosenbluth J (1973) Postjunctional membrane specialization at cholinergic myoneural junctions in the leech. J Comp Neurol 151:399–406

Satir P, Gilula NB (1973) The fine structure of membranes and intercellular communication in insects. Annu Rev Entomol 18:143–166

Stewart WW (1978) Intracellular marking of neurons with a highly fluorescent naphthalamide dye. Cell 14:741–759

Thompson WJ, Stent GS (1976a) Neuronal control of the heartbeat in the medicinal leech. I. Generation of the vascular constriction rhythm by heart motor neurons. J Comp Physiol 111:261–279

Thompson WJ, Stent GS (1976b) Neuronal control of the heartbeat in the medicinal leech. II. Intersegmental coordination of heart motor neuron activity by heart interneurons. J Comp Physiol 111:281–307

Thompson WJ, Stent GS (1976c) Neuronal control of the heartbeat in the medicinal leech. III. Synaptic relations of heart interneurons. J Comp Physiol 111:309–333

Tulsi RS, Coggeshall RE (1971) Neuromuscular junctions on the muscle cells in the central nervous system of the leech, *Hirudo medicinalis*. J Comp Neurol 141:1–16

Wallace BG (1981a) Distribution of AChE in cholinergic and non-cholinergic neurons. Brain Res 219:190–195

Wallace BG (1981b) Neurotransmitter chemistry. In: Muller KJ, Nicholls JG, Stent GS (eds) Neurobiology of the leech. Cold Spring Harbor Laboratory, New York, pp 147–172

Wallace BG, Gillon JW (1982) Characterization of acetylcholinesterase in individual neurons in the leech central nervous system. J Neurosci 2:1108–1118

Yaksta-Sauerland BA, Coggeshall RE (1973) Neuromuscular junctions in the leech. J Comp Neurol 151:85–100